The Four-Connected Net in the $CeCu_2$ Structure and Its Ternary Derivatives. Its Electronic and Structural Properties

Gerhard Nuspl,[†] Kurt Polborn,[†] Jürgen Evers,*[,†] Gregory A. Landrum,[‡] and Roald Hoffmann*[,‡]

Department of Chemistry and Materials Science Center, Cornell University, Ithaca, New York 14853, and Institut für Anorganische Chemie der Universität München, Meiserstrasse 1, D-80333 München, Germany

Received March 7, 1996[⊗]

The crystallochemistry of and the bonding in the orthorhombic four-connected nets of $BaIn_2$ ($CeCu_2$ structure) and of CaPtSn (TiNiSi structure, a derivative of the $CeCu_2$ structure) are analyzed with approximate molecular orbital calculations. Following the Zintl concept, in $BaIn_2$ the In^- ions are isoelectronic with group IV tin and should adopt a four-connected structure. In contrast to α-tin, which has a cubic diamond structure, the indium ions in $BaIn_2$ build up an orthorhombic three-dimensional four-connected net containing distorted tetrahedra and ladder polymers of four-membered rings. In the $CeCu_2$ structure (space group *Imma*) two bond angles in these distorted tetrahedra are fixed at 90°. The four-connected net in the $CeCu_2$ structure is topologically related to the layers in black phosphorus (space group Cmca). In CaPtSn (TiNiSi structure) the orthorhombic four-connected net is formed by $(PtSn)^{2-}$ ions in an ordered arrangement. Calculations on $BaIn_2$ and CaPtSn show that the four-connected nets are increasingly stabilized as the valence electron count is increased from 16 to 30 valence electrons per 4 formula units. For more than 30e, the nets are destabilized due to filling of M−E antibonding states. Structural data obtained by precise single crystal investigations for the TiNiSi series CaPdIn (20e), CaPdSn (24e), CaPdSb (28e), and CaAgSb (32e), confirm the results of the extended Hückel calculations. We find an interesting and understandable angular asymmetry of the tetrahedral sites in these ternary compounds.

1. Introduction

A number of intriguing three-dimensional four-connected (3D4C) nets can be derived by joining puckered two-dimensional three-connected layers, such as the one shown in two views in **1** and **2**. In the elemental α-arsenic structure[1]

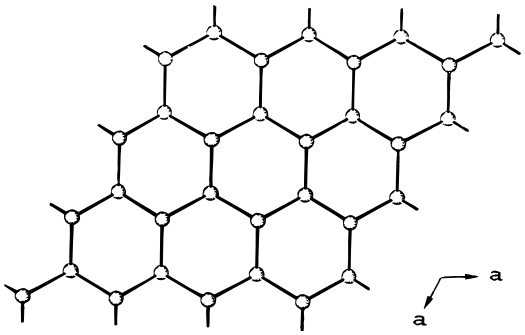

1

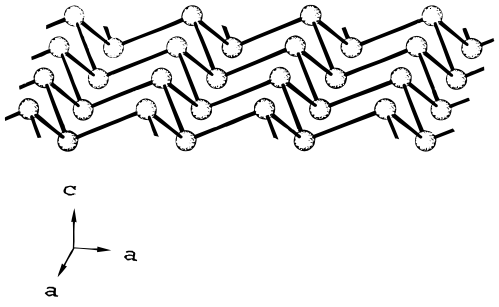

2

(3) (space group $R\bar{3}m$) with layer sequence ABC, each layer

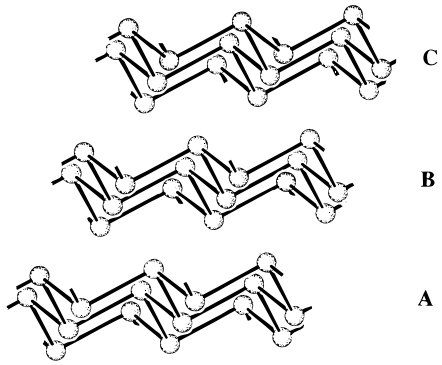

3

consists of six-membered rings in the chair conformation. Due to the highly symmetric arrangement of "up" and "downs" (here the reference is to the element−element bonds) in point group $\bar{3}m$, the bonds in this structure are all equal in length and the bond angles are equal as well (As: 2.517 Å, 96.6°, respectively).[2]

The cubic 3D4C net of diamond[3] **(4)** (space group $Fd\bar{3}m$, but a trigonal setting in subgroup $R\bar{3}m$ is also possible) can be derived from three layers of α-arsenic. Layers B and C in diamond are shifted relative to the α-arsenic stacking so that tetrahedral coordination is created (a "down" of one layer above an "up" of the layer below).

[†] Universität München.
[‡] Cornell University.
[⊗] Abstract published in *Advance ACS Abstracts,* October 1, 1996.

(1) Bradley, A. J. *Philos. Mag.* **1924**, *47*, 657.
(2) Villars, P.; Calvert, L. D. *Pearson's Handbook of Crystallographic Data for Intermetallic Phases,* 2nd ed.; American Society for Metals: Metals Park, OH, 1991.
(3) Bragg, W. H.; Bragg, W. L. *Nature* **1913**, *91*, 557. *Proc. R. Soc. London* **1913**, *89A*, 277.

S0020-1669(96)00255-8 CCC: $12.00

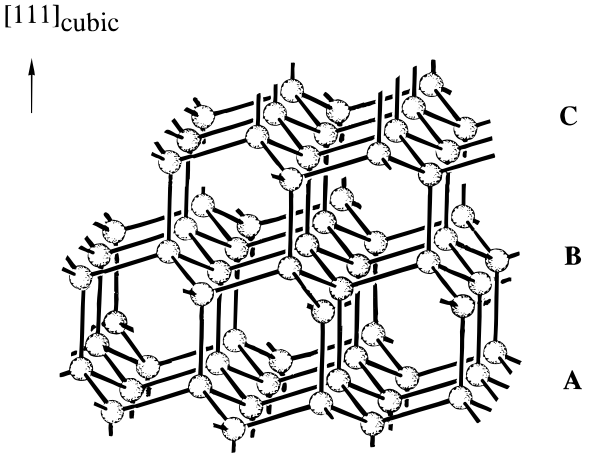

4

There is a rare hexagonal 3D4C carbon allotrope, lonsdaleite[4] (**5**, space group $P6_3/mmc$) with layer sequence AB. Lonsdaleite

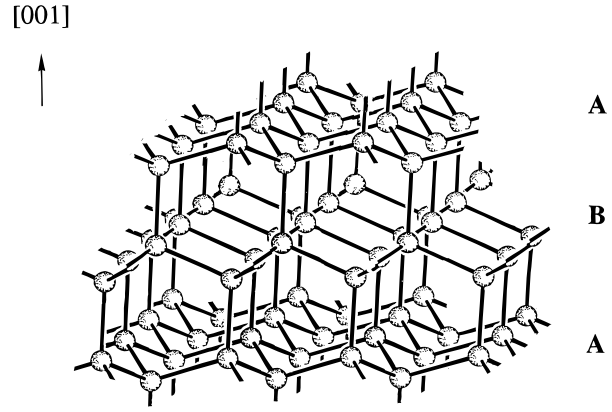

5

is obtained from α-arsenic layers (sequence AA) if every second layer is rotated by 60° and adjusted so that tetrahedral coordination is obtained. The bond distances and bond angles in this hexagonal 3D4C net are ideal (as in the cubic case) if the axial ratio (c/a) is 1.633. In this case as well as in the cubic net, a packing density of 34.01% (half the filling of the body-centered cubic packing) is achieved.

There are many binary realizations of the diamond and lonsdaleite structures in polymorphs of the zincblende and wurtzite structure types. These cubic and hexagonal 3D4C nets have also been observed in Zintl-phases and intermetallic compounds. The cubic net is found for a 1:1 composition in the NaTl structure[5] **(6)** (space group $Fd\bar{3}m$) and for 1:2-composition (ternary phases) in the MgAgAs[6] **(7)** and the LiAlSi[7] **(8)** structures (space group for both: $F\bar{4}3m$—LiAlSi-type shown for $MgAuSn$[2]).

While the hexagonal 3D4C net has not yet been realized for a 1:1-stoichiometry, there are some examples for 1:2 composition: a binary version in the $CaIn_2$[8] **(9)** structure (space group $P6_3/mmc$) and a ternary one for the LiGaGe[9] structure (space group $P6_3mc$).

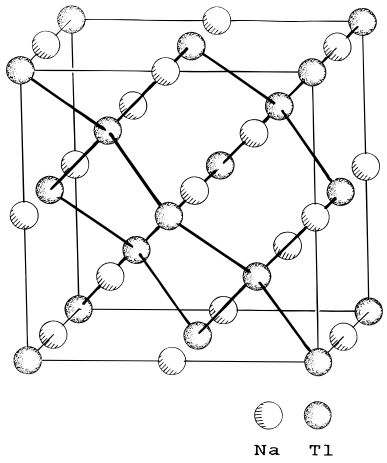

6

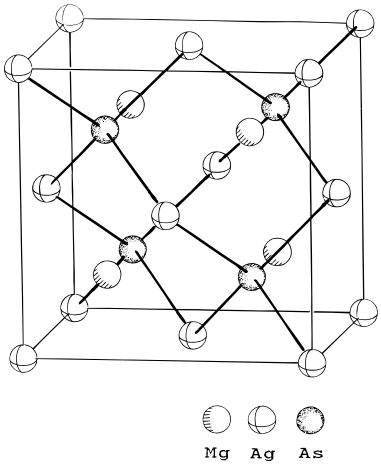

7

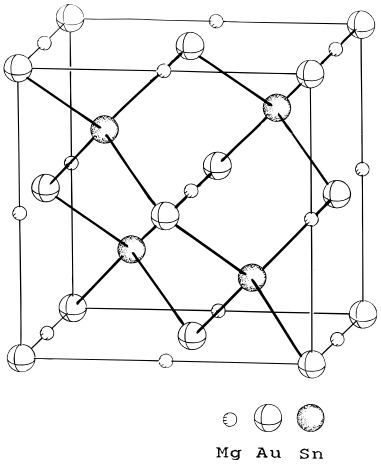

8

Interestingly, an orthorhombic 3D4C net of lower symmetry (space group Imma) can be achieved by joining three-connected layers of black phosphorus[10] **(10**, **11)** (space group *Cmca*). Zigzag chained "ups" are bonded to zigzag chained "downs", forming layers of six-membered chairs, too. These layers in black phosphorus show only mmm point symmetry. Therefore the structure contains two different bond lengths (2 + 1:

(4) Bundy, F. P.; Kasper, J. S. *J. Chem. Phys.* **1967**, *46*, 3437.
(5) Zintl, E.; Dullenkopf, W. *Z. Phys. Chem.* **1932**, *B16*, 195.
(6) Nowotny, H.; Sibert, W. *Z. Metallk.* **1941**, *33*, 391.
(7) Schuster, H.-U.; Hinterkeuser, H.-U.; Schäfer, W.; Will, G. *Z. Naturforsch.* **1965**, *31B*,1540.
(8) Iandelli, A. *Z. Anorg. Allg. Chem.* **1964**, *330*, 221.
(9) Bockelmann, W.; Schuster, H.-U. *Z. Anorg.Allg.Chem.* **1974**, *410*, 233.
(10) Brown, A.; Rundquist, S. *Acta Crystallogr*. **1965**, *19*, 684.

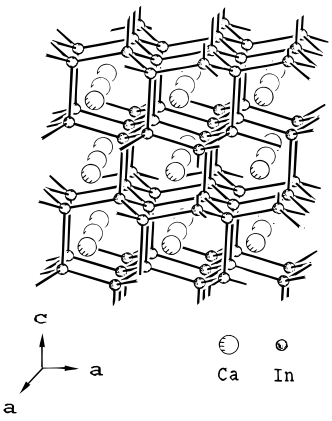

9

2.224 Å 2×, 2.245 Å 1×) and two different bond angles (2 + 1: 102.1° 2×, 96.3° 1×).[2] In such tilted chairs there is no

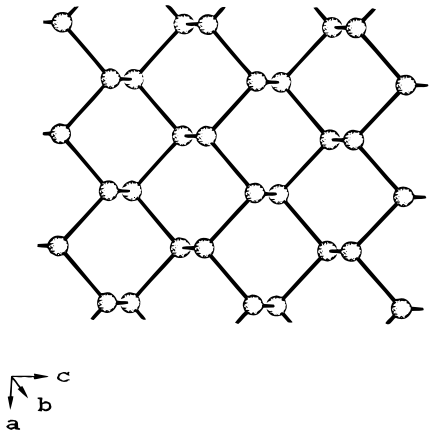

10

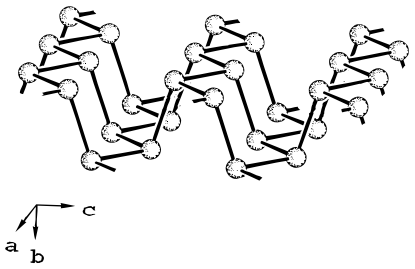

11

comfortable "resting" and "dreaming" as there was in those arsenic layers we saw above. It is as if one has moved up the chairs in order to clean the floor!

To build up the new 3D4C net by stacking layers of the black phosphorus type, the original layer sequence AB has to be changed. In black phosphorus an "up−down" edge of a six-membered ring of layer A lies above the center of a six-membered ring of layer B. In the resulting orthorhombic 3D4C net **(12**, **13)**, six-membered chairs lie directly above each other, but in such a way that groups of three connected "downs" are joined to three-connected "ups" of the layer below. Due to this kind of joining in the orthorhombic 3D4C net, there arise three different bond lengths (2 + 1; 1) and four different bond angles (2 + 1; 2; 1). A consequence of creating a fourth bond between zigzag chained "ups" and "downs" in parallel planes is that two of the three new bond angles take on a value of 90°.

This unusual structure features "ladders" of four-membered rings. Now four-membered rings are substantially strained in

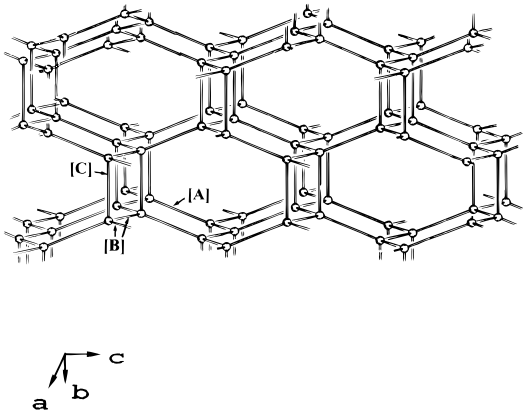

12

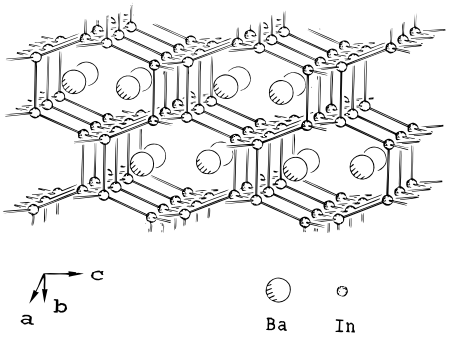

13

carbon chemistry and are not often seen in other group IV element structures. Indeed, up to now this orthorhombic 3D4C net has not been observed in any elemental structure. In addition, the space filling of this net is about 30%, which is quite a bit lower than the value of 34.01% for the two diamond-type nets.

If one departs from the elements, the situation changes dramatically, for just this 3D4C net turns out to be quite common. It is found in the binary $CeCu_2$ structure[11] (**13**, space group *Imma*—shown here for $BaIn_2$) and in ternary derivatives in the TiNiSi structure[12] (space group *Pnma*). In fact, as of 1991,[2] the TiNiSi structure has been recognized for more than 300 ternary MTX phases, while the $CeCu_2$ type is known for more than 50 binary intermetallics MT_2 and a few Zintl-phases MX_2 (M, alkaline earth or rare earth metal; T, late transition metal, including Zn, Cd, and Hg; X, main group element). So this is hardly a rare structure.

The orthorhombic 3D4C net may be obtained in an equilibrium transformation at high pressures and high temperatures (4 GPa, 1000 °C), starting with a net that can be considered to be a three-connected analogue of the cubic diamond net. In a belt apparatus, CaPtSi-I[13] ($LaIrSi$[14] structure) with an ordered three-connected net of Pt and Si atoms is obtained as a quenchable CaPtSi-III[15] polymorph (TiNiSi structure) possessing the orthorhombic 3D4C net.

The bonding and electronic properties of some binary and ternary phases with three-connected nets have been analyzed in detail by R.H.[16] Lee, using the "second moment equalization

(11) Larson, A. C.; Cromer, D. T. *Acta Crystallogr.* **1961**, *14*, 73.
(12) Shoemaker, C. B.; Shoemaker, D. P. *Acta Crystallogr.* **1965**, *18*, 900.
(13) Evers, J.; Oehlinger, G. *J. Solid State Chem.* **1986**, *62*, 133.
(14) Klepp, K.; Parthé, E. *Acta Crystallogr.* **1982**, *B38*, 1541.
(15) Evers ,J.; Oehlinger, G.; Polborn, K.; Sendlinger, B. *J. Solid State Chem.* **1993**, *103*, 45.
(16) Zheng, C.; Hoffmann, R. *Inorg. Chem.* **1989**, *28*, 1074.

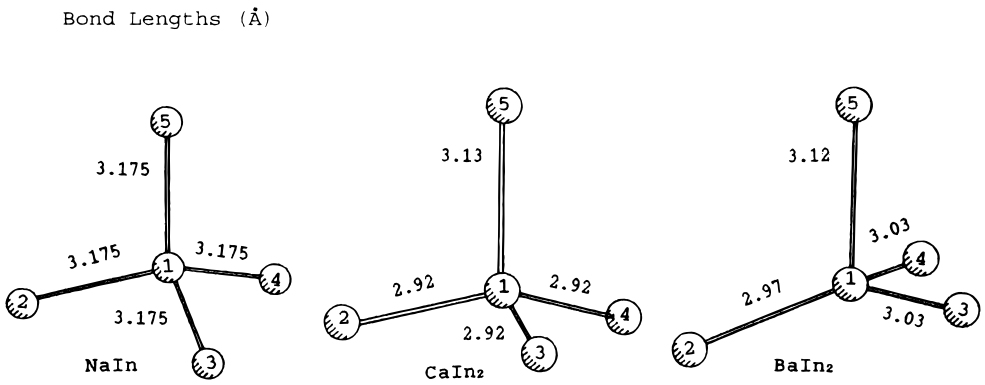

Bond Angles (°)	NaIn	$CaIn_2$	$BaIn_2$
213	109.5	113.8	118.1
314	109.5	113.8	118.5
214	109.5	113.8	118.1
215	109.5	104.6	112.8
315	109.5	104.6	90
415	109.5	104.6	90

Figure 1. Increase in angular distortion in the In−tetrahedra, going from NaIn (T_d), to $CaIn_2$ (C_{3v}) and then to $BaIn_2$ (C_s). Labeling of tetrahedra atoms, bond lengths (Å) and bond angles (deg) are also given.

method", has carried out calculations[17] on 10 structural types of main group intermetallic compounds (including the $CaIn_2$, $CeCu_2$, and MgAgAs structures) and perceptively analyzed their relative stabilities.

In this contribution we will explore the bonding and structural properties of 3D4C nets in MX_2, MT_2, and MTX compounds with the $CeCu_2$ and TiNiSi structures. All calculations have been performed using the extended Hückel implementation of the tight-binding method.[18,19]

2. NaIn, $CaIn_2$, and $BaIn_2$

The binary compounds $CaIn_2$,[8] $SrIn_2$[8], and $BaIn_2$[20] are Zintl-phases.[21] According to Zintl's simple but extremely useful concept, the electropositive Ca, Sr, and Ba atoms donate both of their two valence electrons to the more electronegative In. Thus Ca^{2+}, Sr^{2+}, Ba^{2+}, and 2 In^- are formally created. The In^- ions are isoelectronic to Sn (main group IV), which crystallizes in a diamond structure in the α-Sn modification. Therefore, following Zintl's idea,[21] four-connected In^- nets are expected for $CaIn_2$, $SrIn_2$, and $BaIn_2$, with the Ca^{2+}, Sr^{2+}, and Ba^{2+} counterions filling the cavities of the nets. In fact, $CaIn_2$ and $SrIn_2$ crystallize with the hexagonal 3D4C net of the $CaIn_2$ structure, while $BaIn_2$ assumes the orthorhombic 3D4C net of the $CeCu_2$ structure which we drew above.

Interestingly, a cubic 3D4C net of In^- ions also exists. In NaIn[22] (NaTl structure) all In−In bonds are of equal length (3.175 Å)[2] and form the same angles (109.5°). However, the symmetry of the In^- nets is lowered in $CaIn_2$ and $BaIn_2$. In the hexagonal 3D4C net of $CaIn_2$,[23] one finds an axial ratio $c/a = 1.58$ ($(c/a)_{ideal} = 1.633$) and a positional parameter $z = 0.452$ ($z_{ideal} = 0.4375 = {}^7/_{16}$) in the hexagonal 3D4C net. The resulting bond distances are 2.92 Å (3×) and 3.13 Å (1×). The bond angles within the distorted tetrahedra separate into two groups of 113.8° (3×) and 104.6° (3×), with an average value of 109.2°. This average value is very close to the ideal value of 109.5°. The distortion of the hexagonal 3D4C net is probably influenced by the Ca^{2+} ions, which fill the cavities of the four-connected net.

In $SrIn_2$[24] ($CaIn_2$ structure) the In^- bond distances are increased to 2.98 Å (3×) and 3.30 Å (1×). As the cation radius increases from $r_{Ca^{2+}} = 0.99$ Å to $r_{Sr^{2+}} = 1.12$ Å, the long In−In bond in the net expands from 3.13 Å ($CaIn_2$) to 3.30 Å ($SrIn_2$). Therefore one can estimate (taking $r_{Ba^{2+}} = 1.34$ Å) a value of at least 3.40 Å for the long bond distance of $BaIn_2$ in the $CaIn_2$ structure. This bond distance is too long for a In−In single bond. $BaIn_2$ abandons the $CaIn_2$ structure and favors the orthorhombic 3D4C net of the $CeCu_2$ structure. Here the In−In bonds are shorter than those in $SrIn_2$ ($CaIn_2$ structure): 2.97 Å (1×), 3.03 Å (2×), and 3.12 Å (1×).[25] However, the bond angles within the "tetrahedra" are distorted to 118.1° (2×), 118.5° (1×), 112.8° (1×), and 90° (2×). At the price of creating two 90° bond angles, relatively short In−In bonds and large cavities for the Ba^{2+} ions are formed in the four-connected net. In comparison to black phosphorus, the puckering of the indium layers in the orthorhombic 3D4C net of $BaIn_2$ is reduced. Otherwise the cavities in the net would be too small for two Ba^{2+} counterions to be well accommodated.

(17) Lee, S. *J. Am. Chem. Soc.* **1991**, *113*, 101.
(18) Hoffmann, R. *J. Chem. Phys.* **1963**, *39*, 1397.
(19) Landrum, G. *YAeHMOP* ("Yet Another extended Hückel Molecular Orbital Package"), Version 0.1a, 1994. *YAeHMOP* is available on the World Wide Web at
http://overlap.chem.cornell.edu:8080/yaehmop.html
(20) Bruzzone, G.; Bonino, G. B. *Atti Accad. Nat. Lincei* **1970**, *48*, 235.
(21) Schäfer, H.; Eisenmann, B.; Müller, W. *Angew. Chem.* **1973**, *85*, 742. *Angew. Chem. Int. Ed. Engl.* **1973**, *12*, 694.
(22) Zintl, E.; Neumayr, S. *Z. Phys. Chem.* **1933**, *B20*, 272.
(23) Nuspl, G. Dissertation, Universität München, 1996. Refinement of the structural data for $CaIn_2$: Guinier diffractometer Mo $K_{\alpha 1}$; quartz monochromator, $\theta = 3-18°$; increment 0.02°; 750 data points; Rietveld method, $R_{Prof} = 6.7\%$; *a*, *c* = 4.891(1), 7.736(2) Å; $z_{In} = 0.452(1)$.
(24) Nuspl, G. Dissertation, Universität München, 1996. Refinement of the structural data for $SrIn_2$ ($CaIn_2$ structure): Guinier diffractometer, as mentioned above; $R_{Prof} = 11.9\%$; *a*,*c* = 5.006(1), 8.055(2) Å; $z_{In} = 0.455(1)$.
(25) Nuspl, G. Dissertation, Universität München, 1996. Refinement of the structural data for $BaIn_2$ ($CeCu_2$ structure):Guinier diffractometer, as mentioned above, $R_{Prof} = 5.4\%$; $a = 5.207(1)$ Å, $b = 8.523(2)$Å, $c = 8.561(2)$ Å, $z_{Ba} = 0.551(1)$, $y_{In} = 0.067(1)$, $z_{In} = 0.160(1)$.

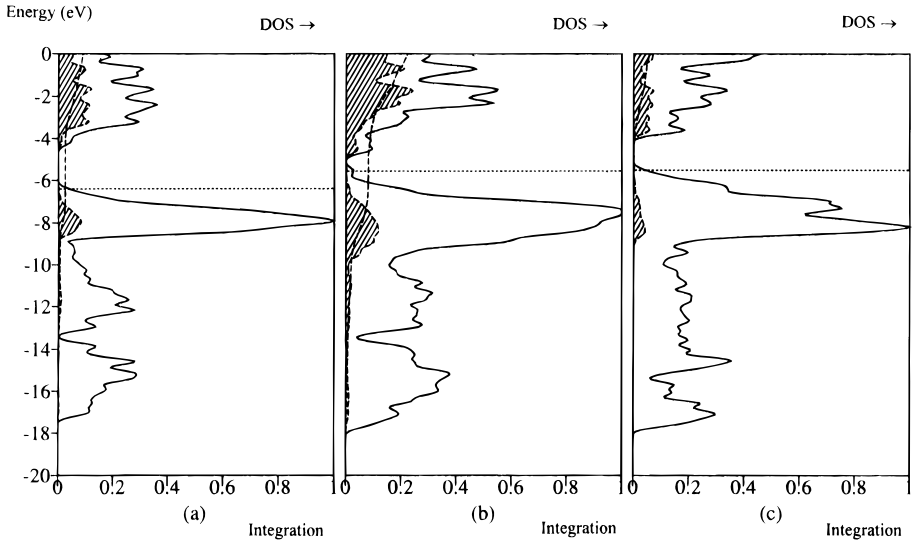

Figure 2. (a) Density of states (DOS) of NaIn: shaded, contribution from sodium; dashed line, integration of sodium on a scale of 0−1; solid line, total DOS. (b) Density of States (DOS) of $CaIn_2$: shaded, contribution from calcium; dashed line, integration of calcium on a scale of 0−1; solid line, total DOS. (c) Density of states (DOS) of $BaIn_2$: shaded, contribution from barium; dashed line, integration of barium on a scale of 0−1; solid line, total DOS.

Let us see how the geometrical features of these structures might influence their electronic properties. In each structure (NaIn, $CaIn_2$, $BaIn_2$) every In^- is surrounded by four other In^- in an exactly or approximately tetrahedral arrangement. The distortion increases on going from NaIn (cubic 3D4C net) to $CaIn_2$ (hexagonal 3D4C) and to $BaIn_2$ (orthorhombic 3D4C net). In Figure 1 the local tetrahedral environments in these structures are compared.

MO calculations for molecular models of ideal tetrahedra (NaIn) with T_d symmetry and the distortion to C_{3v} ($CaIn_2$) and C_s ($BaIn_2$) symmetry show that the positions of the A_1 and T_2 energy levels of ideal tetrahedra are not appreciably changed, though the degeneracies are predictably lowered in the distorted tetrahedra.

The four-connected In^- nets in NaIn, $CaIn_2$, and $BaIn_2$ are formally saturated. Therefore from a chemical point of view, one would expect semiconducting properties for these three compounds, at least for NaIn in the cubic NaTl structure.[22] In NaIn the ideal tetrahedra of In^- are isosteric with those of group IV α-Sn, a semiconductor with a small gap of 0.08 eV.[26] In addition, one would expect a gap larger than 0.08 eV in NaIn, as sodium and indium show a great difference in electronegativity.

In Figure 2a the density of states (DOS), computed using the extended Hückel method,[18,19] is shown for NaIn, in Figure 2b for $CaIn_2$ and in Figure 2c for $BaIn_2$. The solid lines indicate the total DOS, the shaded areas the contributions from sodium, calcium and barium, respectively. In Figure 2a−c the lower lying bands (centered at around −15 eV) are, as expected, mainly composed of indium s states, while the upper ones arise from the p bands of indium. In all three compounds NaIn, $CaIn_2$, and $BaIn_2$, the alkaline metal and the alkaline earth metal ion's orbitals do not play a significant role in the covalent bonding. The small total population of Na, Ca, and Ba (0.20, 0.65 and 0.01 electrons, respectively) supports the Zintl ionic formulation.

For the less ionic compound $CaIn_2$ no substantial gap is recognizable between the valence and conduction bands (Figure 2b), which indicates semimetallic properties. For the more ionic compounds NaIn and $BaIn_2$, gaps of approximately 1.5 eV (Figure 2a) and 1.0 eV (Figure 2c) have been calculated. However, experience has shown that overly large gaps are predicted for ionic compounds by using the extended Hückel molecular orbital method. Indeed, band structure calculations for NaIn using the relativistic plane wave (RAPW) method indicated semimetallic properties.[27] In a qualitative view the DOS graphs of the cubic NaIn and the hexagonal $CaIn_2$ are very similiar to the less symmetric orthorhombic $BaIn_2$ (Figures 2a−c). Nevertheless we have performed a detailed analysis of the bonding properties in the orthorhombic 3D4C net of $BaIn_2$.

In order to estimate the relative strengths of the bonds in this net, crystal overlap population (COOP) curves[28] have been calculated for the indium net in $BaIn_2$. To allow a fair comparison, all four bonds have been fixed to their average length of 3.03 Å. The bond angles in the distorted tetrahedra remain at their experimentally determined values (Figure 1).

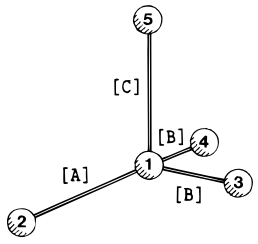

14

The bond between atoms 1 and 2 in the distorted tetrahedra is labeled **[A]**, the bonds between 1−3 and 1−4 **[B]**, and the bond between 1−5 **[C]** (see Figure 1 and structure **14**). The COOP curves for bond **[A]**, bonds **[B]**, and bond **[C]** in the $BaIn_2$ structure are shown in Figure 3a−c. Positive regions indicate bonding; negative regions, antibonding.

Inspection of Figure 3a shows that the occupied states are consistently bonding for bond **[A]** up to the Fermi level. Only a very small group of states near the Fermi level has a negative contribution to the COOP. Bonds **[B]** (Figure 3b) are characterized by a larger negative COOP region near the Fermi level. Thus, by filling the net with 32 electrons per unit cell we

(26) *Handbook of Chemistry and Physics*, 57th ed., 1976−1977; Weast, R. C., Ed.; CRC Press: Cleveland, OH, 1976; p E-101.

(27) Schmidt, P. C. *Struct. Bonding* **1987**, *65*, 91.

(28) Hughbanks, T.; Hoffmann, R. *J. Am. Chem. Soc.* **1983**, *105*, 3528.

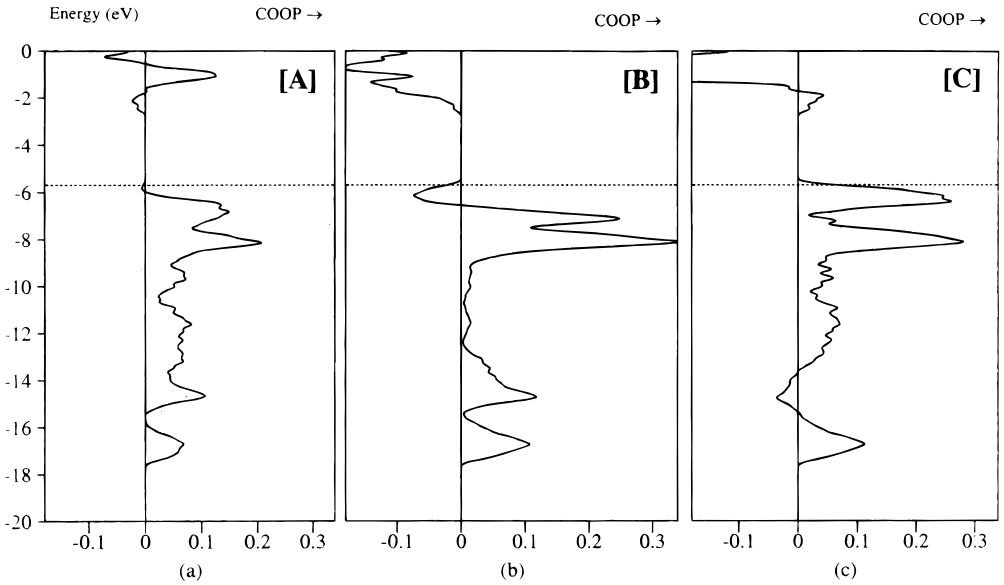

Figure 3. Crystal orbital overlap population (COOP) curves for (a) bond **A** (b) bonds **B**, and (c) bond **C** in the **ideal** indium−net of $BaIn_2$. The Fermi level for the system with 32 electrons per unit cell is indicated by a dotted horizontal line.

populate a substantial number of antibonding states for bonds **[B]**. Since there are two type **[B]** bonds in the distorted tetrahedron (Figure 1 and **14**), this destabilization of **[B]** will strongly influence the stability of the whole net. Bond **[C]** (Figure 3c) shows a large positive overlap population peak near the Fermi level. States in this region, slightly bonding in **[A]** and antibonding in **[B]**, are strongly bonding in **[C].**

Interestingly, the negative COOP region for bonds **[B]** near the Fermi level is strongly influenced by the interlayer distance of the phosphorus-like sheets (bond **[C]**). For longer (hypothetically) interlayer distances, the negative COOP region for bonds **[B]** strongly decreases.

What is the orbital origin of this region of antibonding in the **[B]** type bond just below the Fermi level? Our curiosity piqued by this finding, we have gone back (because these are Zintl-phases after all) to an organic analogue: the cyclobutane ladder polymer (stoichiometry CH, unit cell $(CH)_4$) **15**. Figure 4 shows

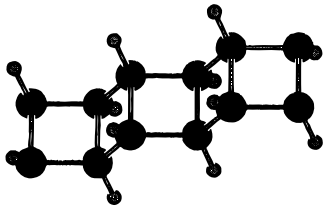

15

the calculated COOPs for this one-dimensional insulating polymer. Note the same feature we had for the In^- net: a set of states just below the Fermi level which are bonding in the **[C]** bond and antibonding in the **[B]** bond. What are these high lying orbitals? A representative one—really the highest lying σ orbital of the polymer—is shown schematically in **16**. Note

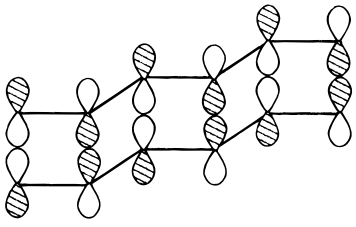

16

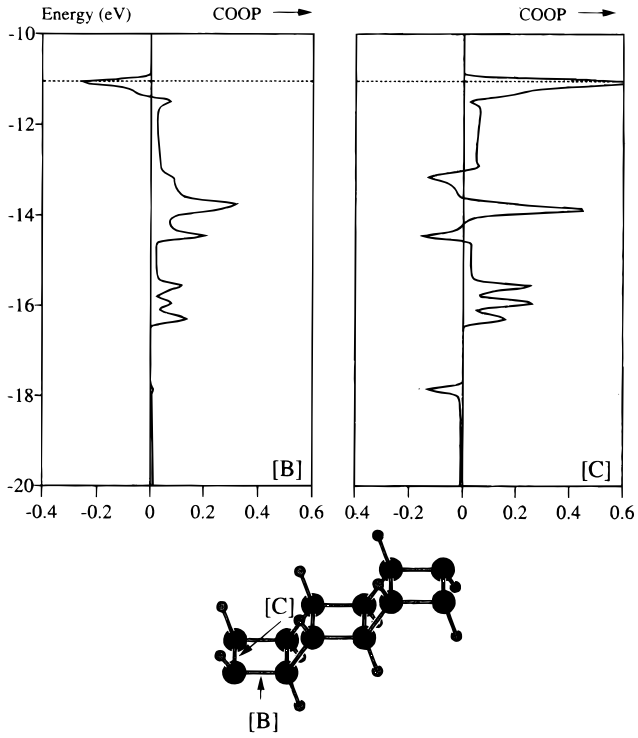

Figure 4. Crystal orbital overlap population (COOP) curves for bond **B** and bond **C** in the cyclobutane ladder polymer (stoichiometry CH, unit cell $(CH)_4$). The Fermi level for the system is indicated by a dotted horizontal line.

how this level is σ bonding in the **[C]** type bond (vertical) and π antibonding in the **[B]** type bond (horizontal). It may be derived from the very highest π orbital of a polyacetylene chain which could be thought of as "half" of the ladder polymer.

To show the effect of the number of valence electrons on the stabilities of bonds **[A]**, **[B]**, and **[C]**, average overlap populations have been calculated for various electron counts for the In^- net in $BaIn_2$ (Figure 5). Figure 5 shows that from 20 to 28 electrons the average overlap population increases in the sequence **[C]**, **[B]**, **[A]**. Therefore in this region bond **[C]** is expected to be the longest, bonds **[B]** of medium length, and bond **[A]** the shortest. At 28 electrons the graphs for **[A]** and

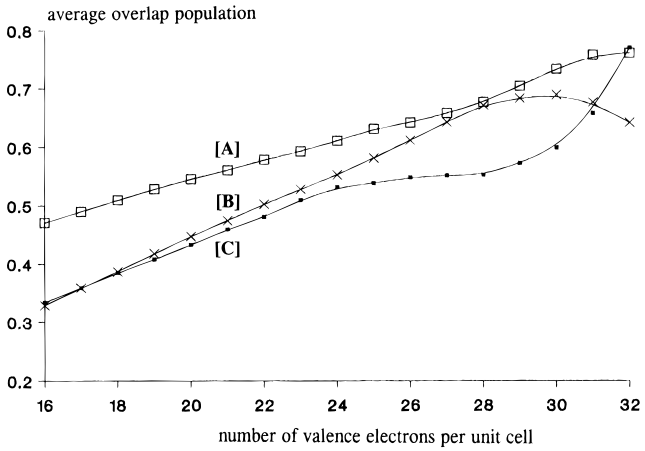

Figure 5. Average overlap population as a function of the number of valence electrons per unit cell with four formula units for the ideal In^- net of $BaIn_2$.

[B] nearly touch each other; near this electron count bonds **[A]** and **[B]** should be approximately equal in length.

At approximately 30e the **[B]** bonds have their highest average overlap population. For higher electron concentrations, the average overlap population for **[B]** decreases due to population of antibonding levels. Therefore, the highest stability for the orthorhombic 3D4C net should be at 30e per unit cell or 7.5e per formula unit. This is in good agreement with the results of Lee[17] who derived a stability maximum for the $CeCu_2$ structure with 7e per formula unit.

Additionally it is also shown that stabilization of the interlayer bond **[C]** in the region between 31 and 32 e (Figure 5) is associated with a weakening of the intralayer bonds **[B]**.

Average overlap population trends have also been calculated for two other isotypic compounds in the $CeCu_2$ structure: $SrAl_2$[29,30] and $Eu^{II}Ga_2$.[8,31,32] For up to 30 valence electrons, the graphs for the **[A]**, **[B]**, and **[C]** type bonds in the Al^- and Ga^- nets show the same tendencies as for the In^- net: all three bonds are stabilized up to 30e and bond **[B]** is destabilized in the region from 30 to 32e.

It must be mentioned that the overlap population curves were calculated using the structural parameters observed for phases with 32 electrons. In the orthorhombic 3D4C net only two bond angles are fixed at 90° by symmetry (Figure 1); four bond angles and the bond distances are variable. If the number of valence electrons is varied by changing the composition MX_2 or MT_2, the ratio of the orthorhombic lattice parameters and also the positional parameters should (and do) show variation. Therefore only general trends can be derived from such graphs.

3. Binary Compounds with the $CeCu_2$ Structure

The alphabetic listing of compounds with the $CeCu_2$ structure published in 1991 contains 61 binary phases.[2] In Table 1, we list the 24 binary compounds with monovalent alkali metal and divalent alkaline earth metal or divalent rare earth metal cations which are known to adopt the $CeCu_2$ structure.[2]

With trivalent earth or rare earth metals there are 36 phases, distributed in number as follows: $M^{III}Cu_2$, 12, $M^{III}Ag_2$, 4; $M^{III}Au_2$, 3; $M^{III}Zn_2$, 13; $M^{III}Ga_2$, 3; $M^{III}In_2$, 1. $PuCu_2$ crystallizes with the $CeCu_2$ structure, too, but here the oxidation state of plutonium is unknown.

Table 1. Binary Compounds with $CeCu_2$ Structure[2] Containing Monovalent Alkali Metal or Divalent Alkaline Earth or Divalent Rare Earth Metal Cations

composition and no. of compounds									
16 VE[b]		20 VE		24 VE		28 VE		32 VE	
$M^{II}Cu_2$:	2	$M^{I}Hg_2$:	1	$M^{II}Zn_2$:	3			$M^{II}Al_2$:	1
$M^{II}Ag_2$:	5			$M^{II}Cd_2$:	4			$M^{II}Ga_2$:	1
$M^{II}Au_2$:	4			$M^{II}Hg_2$:	2			$M^{II}In_2$:	1
Σ:	11[a]	Σ:	1	Σ:	9	Σ:	0	Σ:	3

[a] Σ = total number of compounds. electron count: M^I, 1; M^{II}, 2; Al, Ga, In, 3; Cu, Ag, Au (d^{10}) + 1; Zn, Cd, Hg (d^{10}) + 2. [b] VE = valence electrons per unit cell.

For most of these binary compounds, lattice and positional parameters were derived in the 1960s by low resolution techniques, especially from Debye−Scherrer powder photographs.[2] Precise bond distances cannot be reliably obtained from such data. In order to show the variation of bond distances **[A]**, **[B]**, and **[C]** as a function of the number of valence electrons, one needs a homologous series of compounds. Since the bond distances within the 3D4C net are influenced by the size of the constituent elements M,T, or X, their radii must be fixed. If this is impossible, radii have to be changed in small controlled steps. Second, the number of valence electrons needs to be varied over a large range (e.g. 20 to 32e). Lastly, precise structural parameters, derived from single crystal investigations on four-circle diffractometers, are needed. These three demands can be better met in homologous series of ternary compounds of composition MTX with an orthorhombic 3D4C net than in binary ones.

4. Ternary Compounds with the TiNiSi Structure

The TiNiSi structure[12] (space group *Pnma*) is an ordered ternary derivative of the binary $CeCu_2$ structure (space group *Imma*). Up to 1991[2] this structure had been identified for more than 300 MTX phases. It appears that this structure must be quite stable and flexible. More than 100 MTX compounds with the TiNiSi structure have been investigated by Parthé and coworkers[33] in Genève.

The nickel and silicon atoms in the TiNiSi structure build up the orthorhombic 3D4C net in an ordered arrangement. Each Ni has four Si neighbors and vice versa. In comparison to the four-connected transition metal (T) net or main group (X) net of the $CeCu_2$ structure, the four-connected T−X net has slightly lower symmetry due to the splitting of the 8-fold position 8(h) for net-atoms in *Imma* (MT_2,MX_2) into two 4-fold positions 4(c) for the T and the X atoms in *Pnma* (MTX). To change positional parameters from 8(h) in *Imma* into 4(c) (2×) in *Pnma* one has to interchange lattice parameters a and b and also positional parameters *x* and *y* and shift the origin.[33]

The T−X bond distances in the TiNiSi structure show the same symmetry properties as the T−T or X−X distances in the $CeCu_2$ structure: bond distance **[A]** appears one time, bond distance **[B]** two times and bond distance **[C]** one time. However, two different distorted tetrahedra (TX_4 and XT_4) are present in the 3D4C T−X nets of MTX phases in the TiNiSi structure. This gives rise to 2 × 6 bond angles. The constraint that two bond angles be 90° in the TX_4 or XT_4 tetrahedra is lost as well. In the MTX compounds there are four bond angles which are only "near" 90°.

(29) Nagorsen, G.; Posch, H.; Schäfer, H.; Wei*β*, A. *Z. Naturforsch.* **1969**, *24B*, 191.
(30) Cordier, G.; Czech, E.; Schäfer, H. *Z. Naturforsch.* **1982**, *37B*, 1442.
(31) Buschow, K. H. J.; de Mooij, D. B. *J. Less-Common. Met.* **1984**, *97*, L5.
(32) Nuspl, G. *Dissertation*, Universität München, 1996. Refinement of the structural data for $Eu^{II}Ga_2$: Guinier diffractometer, as mentioned above; R_{Prof} = 6.0%; *a* = 4.646(1) Å, *b* = 7.638(2) Å, *c* = 7.620(2) Å, z_{Eu} = 0.546(2), y_{Ga} = 0.066(2), z_{Ga} = 0.162(2).
(33) Hovestreydt, E.; Engel, N.; Klepp, K.; Chabot, B.; Parthé, E. *J. Less-Common. Met.* **1982**, *85*, 247.

In recent years many MTX phases with the TiNiSi structure have been investigated with single crystals on four-circle diffractometers in the groups of Schuster[34,35] and Mewis[36−38] in Cologne, Merlo[39] in Genova, and our group in Munich,[15,40,41] especially for the composition CaTX with T = Pd, Pt and Ag, Au and X = Al, Ga, In; Si, Ge, Sn; and As, Sb.

Looking for homologous series, one discovers a four-membered CaTX series with the valence electron count increasing from 20 to 32 per unit cell with four formula units (electron count: Pd (d^{10}) + 0, Ag (d^{10}) + 1)

CaPdIn	CaPdSn	CaPdSb	CaAgSb
(20e)	(24e)	(28e)	(32e)

In this case M^{II} = Ca is fixed, T = Pd or Ag (which are neighboring 4d elements), and X are neighboring 5sp main group elements. Therefore the influence of the size of the constituent elements on bond distances is minimized. For the CaTX phases, the series given above is up to now the only one with four members. To the authors' best knowledge there are only three 32 electron $M^{II}TX$ compounds with the TiNiSi structure ($Yb^{II}AgSb$,[39] CaAgSb,[39] MgCuP[36]) and two $M^{I}TX$ compounds (NaCdAs,[35] NaCdSb[42]). In addition, NaAuSn[43] adopts the TiNiSi structure and NaAuSb[44]—quenched from 5 GPa, 800 °C—the $CeCu_2$ structure. Therefore a unique three-membered NaTX series exists with NaAuSn (24e), NaAuSb (28e), and NaCdSb (32e).

Precise single crystal data of the above given CaTX series are taken from the studies of three different research groups,[38,39,41,45] which are presented in Table 2.

In Figure 6 the volume per unit cell is shown as a function of the number of valence electrons per unit cell for the compounds CaPdIn, CaPdSn, CaPdSb, and CaAgSb.

The volume per unit cell in the known compounds shows a drastic increase for electron counts between 28 and 32e: increasing from approximately 269 Å^3 for CaPdX (X = In, Sn, Sb) to 296.9 Å^3 (see Table 2 and Figure 6). This is a change of approximately +9%. The increase in size of the constituent elements on going from CaPdSb to CaAgSb is responsible for a change of approximately +4%.[46] This effect also is observed for $Yb^{II}PdSn$ (262.79 Å^3—24e)[41] and $Yb^{II}AgSb$ (294.31 Å^3—32e).[39] It is evident that CaAgSb and $Yb^{II}AgSb$ with the TiNiSi structure are less densely packed than analogous compounds with 28 or 24e. This is one reason why $M^{II}TX$ and $M^{I}TX$ compounds with this structure are very rare for 32e.

As calculated in Section 2 for the binary compounds, the 3D4C net is stabilized up to 30 and destabilized from 30 to 32 electrons per unit cell. It is interesting to note that this effect is also observed in the extended Hückel calculations for MTX compounds with the TiNiSi structure, e.g. CaPtSn.[47]

Table 2. Structural Data for CaTX Phases with the TiNiSi Structure,[38,39,45] Derived by Single-Crystal Investigations on Four-Circle Diffractometers[a]

	CaPdIn	CaPdSn	CaPdSb	CaAgSb
structure type		TiNiSi		
space group		Pnma		
lattice params				
a (Å)	7.299	7.293	7.354	7.708
b (Å)	4.359	4.572	4.617	4.590
c (Å)	8.490	8.050	7.903	8.393
V[b] (Å^3)	270.1	268.4	268.3	296.9
positional params				
4(c) *x*, $^1/_4$, *z*				
M				
x	0.0314	0.9806	0.0051	0.0173
z	0.6771	0.6851	0.7022	0.6967
T				
x	0.2683	0.2122	0.3160	0.1440
z	0.3712	0.1111	0.4213	0.0661
X				
x	0.1453	0.3356	0.1997	0.2592
z	0.0622	0.4296	0.0939	0.3887

[a] ESDs for lattice parameters, ±0.003 Å; for unit cell volume, 0.1 Å^3; for positional parameters T, X, ±0.0002; Ca, ±0.0005. [b] Per unit cell.

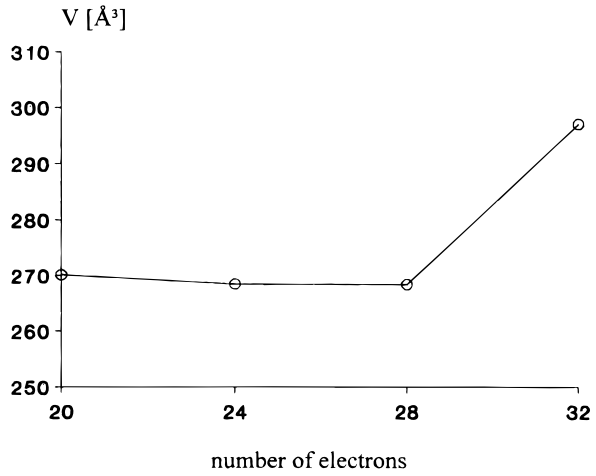

Figure 6. Volume per unit cell (Å^3) for the series of compounds CaPdIn, CaPdSn, CaPdSb, and CaAgSb.

(34) Dascoulidou-Gritner, K.; Schuster, H.-U. *Z. Anorg. Allg. Chem.* **1994**, *620*, 1151.
(35) Krenkel, B.; Tiburtius, C.; Schuster, H.-U. *Z. Naturforsch.* **1979**, *34B*, 1686.
(36) Mewis, A. *Z. Naturforsch.* **1979**, *34B*, 1373.
(37) Johrendt, D.; Mewis, A. *J. Alloys Compd.* **1992**, *183*, 210.
(38) Johrendt, D.; Mewis, A. *Z. Anorg. Allg. Chem.* **1992**, *618*, 30.
(39) Merlo, F.; Pani, M.; Fornasini, M. L. *J. Less-Common. Met.* **1990**, *166*, 319.
(40) Evers, J.; Oehlinger, G.; Polborn, K.; Sendlinger, B. *J. Alloys Compd.* **1992**, 182, L23.
(41) Sendlinger, B. Dissertation, Universität München, 1993.
(42) Savelsberg, G.; Schäfer, H. *Z. Naturforsch.* **1978**, *33B*, 370.
(43) Wrobel, G.; Schuster, H.-U. *Z. Anorg. Allg. Chem.* **1977**, *432*, 95. Although the authors state that NaAuSn is a ternary variant of the $PbCl_2$ structure, they present their structural data in space group $Pna2_1$. This space group is a non-centrosymmetric subgroup of *Pnma* and shows the same extinctions as *Pnma*. For $z = 0$ in $Pna2_1$ the correct setting of NaAuSn is with a center of symmetry in *Pnma* (TiNiSi structure); $a = 7.476$ Å, $b = 4.530$ Å, $c = 8.088$ Å, $x_{Na} = 0.989(2)$, $z_{Na} = 0.664(2)$, $x_{Au} = 0.2067(3)$, $z_{Au} = 0.1303(2)$, $x_{Sn} = 0.3420(5)$, $z_{Sn} = 0.4403(3)$.
(44) Nuspl, G. Dissertation, Universität München, 1996: Guinier diffractometer, as mentioned above; $R_{Prof} = 8.9\%$; NaAuSb, quenched from 5 GPa; 800 °C; $CeCu_2$ structure, space group *Imma*; $a = 4.681(3)$ Å, $b = 7.201(3)$ Å, $c = 8.129(3)$ Å, Na(0, $^1/_4$, 0.52(1)), Au, Sb(0, 0.032-(1), 0.164(1).
(45) Nuspl, G. Dissertation, Universität München, 1996. Refinement of the structural data for CaPdIn: single crystal data, CAD4; Mo Kα, 217 independent reflections [$R_{int} = 7.44\%$]; $R = 3.80\%$, $R_w = 9.43\%$. Only lattice parameters of CaPdIn have been given by: Cirafici, S.; Palenzona, A.; Canepa, F. *J. Less-Common. Met.* **1985**, *107*, 179. Refinement of the structural data for CaPdSn: single crystal data, CAD4; Mo Kα, 211 independent reflections [$R_{int} = 4.44\%$]; $R = 2.37\%$, $R_w = 6.43\%$.
(46) The covalent radii (in Å)—Ca, 1.90 (from bond distances in CaPdX compounds, Table 2); Pd, 1.45;[47,48] Ag, 1.528;[47] Sb, 1.41[47]—have been used to calculate volumes of spheres (in Å^3, Ca, 28.73; Pd, 12.77; Ag, 14.94; Sb, 11.74). With four MTX units per unit cell a volume of 212.96 Å^3 is calculated for CaPdSb and 221.64 Å^3 for CaAgSb. This results in a correction of 1.3% for lattice parameters ($(212.96/221.64)^{1/3} = 0.987$).
(47) The extended Hückel calculations for CaPtSn were performed for CaPtSn instead of CaPdSn, as the tabulated orbital exponents for Pd are probably too contracted (see: Tables of Parameters for Extended Hückel Calculations, collected by Santiago Alvarez, Universitat de Barcelona, June 1989). The crystal data of CaPtSn (*a*, *b*, *c* (Å): 7.314 (1), 4.574(1), 7.930(1))[41] are comparable to those of CaPdSn (Table 2).

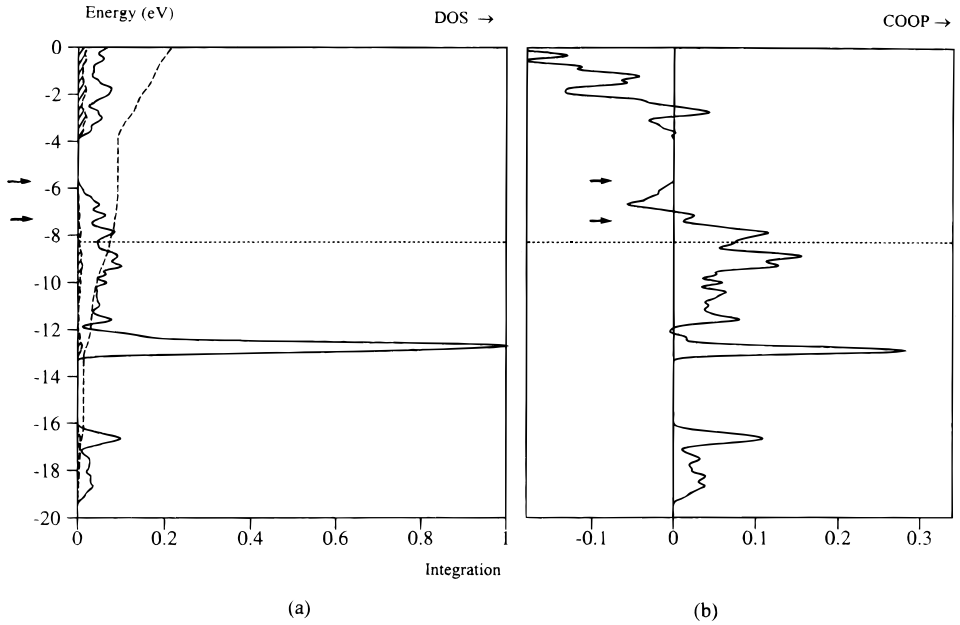

Figure 7. (a) Density of states (DOS) for CaPtSn: solid line, total DOS; shaded, contribution from calcium; dashed line, integration of calcium on a scale of 0−1. (b) Crystal orbital overlap population (COOP) for the Pt−Sn net in CaPtSn. The dotted line indicates the Fermi level for 24e. Two arrows mark the positions of the Fermi level for 28 and for 32e.

Figure 7a shows the DOS for CaPtSn (solid line, total DOS; shaded, contribution from calcium). In Figure 7b some COOP curves for CaPtSn are presented. The Fermi level for 24e is indicated by a dotted line. Two arrows mark the positions of the Fermi level for 28 and 32e respectively.

From inspection of Figure 7a, it is evident that the contributions of divalent calcium to the DOS below E_F are small. In this case the Zintl concept of transferring two electrons from calcium to the more electronegative palladium and tin is a good approximation. The Ca^{2+} counterions do not contribute to covalent bonding: they fill the cavities in the orthorhombic 3D4C $(PtSn)^{2-}$ net and stabilize it electrostatically. In Figure 7a the Fermi level E_F is shown as a dotted horizontal line. A large sharp peak is located about 5 eV below the Fermi level. This peak arises from the d-orbitals of the platinum. Thus, a d^{10} electron count for Pd or Pt is reasonable.

In Figure 7b the COOP curve for the Pt−Sn bond is presented. Positive regions indicate bonding, negative antibonding, as usual. The Fermi level (E_F) shown by the dotted horizontal line is for CaPtSn with 24e. All the levels below this E_F are Pt−Sn bonding. Increasing the number of valence electrons to 28 (as in CaPtSb) continues to populate Pt−Sn bonding states. However, for 32e (as in CaAgSb) one enters a strongly negative region of the COOP curve. Here antibonding is increased and the stability of the bonds within the 3D4C net is diminished.

In Table 3, T−X bond distances (Å) and bond angles (deg) within the distorted TX_4 and XT_4 tetrahedra are shown for CaPdIn, CaPdSn, CaPdSb, and CaAgSb. These data were derived from the results of single crystal investigations using four-circle diffractometers.[38,39,45]

Inspection of Table 3 for the **[A]**, **[B]**, and **[C]** distances in the 3D4C net shows that the average bond length decreases from 2.790 to 2.738 and 2.729 Å, on going from from CaPdIn (20e) to CaPdSn, (24e) and CaPdSb (28e). The average bond length increases to 2.878 Å for CaAgSb (32e). The same trend holds for the series CaPtIn, CaPtSn and CaPtSb, which have been investigated by modern single crystal techniques, as well as for the series NaAuSn, NaAuSb, and NaCdSb. Unfortunately, for $Yb^{II}AgSb$ only lattice parameters have been determined.[39]

Table 3. T−X Bond Distances (Å) and Bond Angles (deg)[38,39,45] within Distorted TX_4 and XT_4 Tetrahedra (Labeling of Atoms within the Distorted Tetrahedra is Given in Figure 1)

	CaPdIn	CaPdSn	CaPdSb	CaAgSb
T−X				
[A] 1−2	2.773	2.717	2.725	2.850
[B] 1−3, 1−4	2.789	2.735	2.684	2.836
[C] 1−5	2.809	2.766	2.824	2.990
av T−X	2.790	2.738	2.729	2.878
TX_4				
213 = 214	128.8	123.1	118.0	114.6
314	102.6	113.4	118.7	108.1
215	120.5	116.1	105.9	100.9
315 = 415	70.2	79.1	93.7	109.1
XT_4				
213 = 214	118.5	117.5	119.7	125.5
314	102.8	113.4	118.7	108.1
215	97.3	102.5	110.7	115.5
315 = 415	109.8	100.9	86.3	70.9

[a] ESDs for bond distances: ±0.002 Å, for bond angles: ±0.2°.

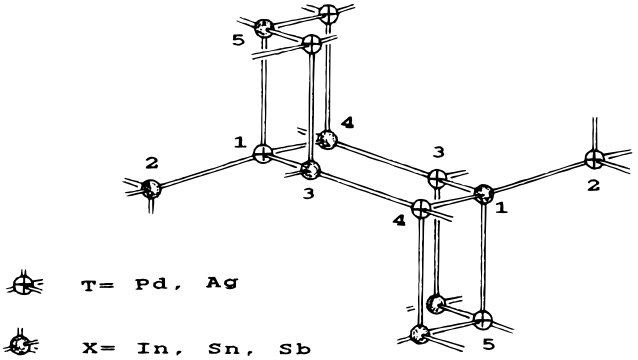

Due to the change in covalent radius on going from Pd (r_{cov} = 1.45 Å[49]) to Ag (r_{cov} = 1.528 Å), one has to adjust the T−Sb bond length in order to be able to comment on the electronically induced structural changes. On going from CaPdSb (2.729 Å Table 3) to CaAgSb (2.878 Å) the correction is estimated as

(48) Pearson, W. B. *The Crystal Chemistry and Physics of Metals and Alloys;* Wiley-Interscience: New York, London, Sydney,Toronto, 1972; p 147. The following covalent radii in Å have been used: Ag, 1.528; In, 1.442; Sn, 1.399; Sb, 1.41; no value for the covalent radius of Pd is tabulated.

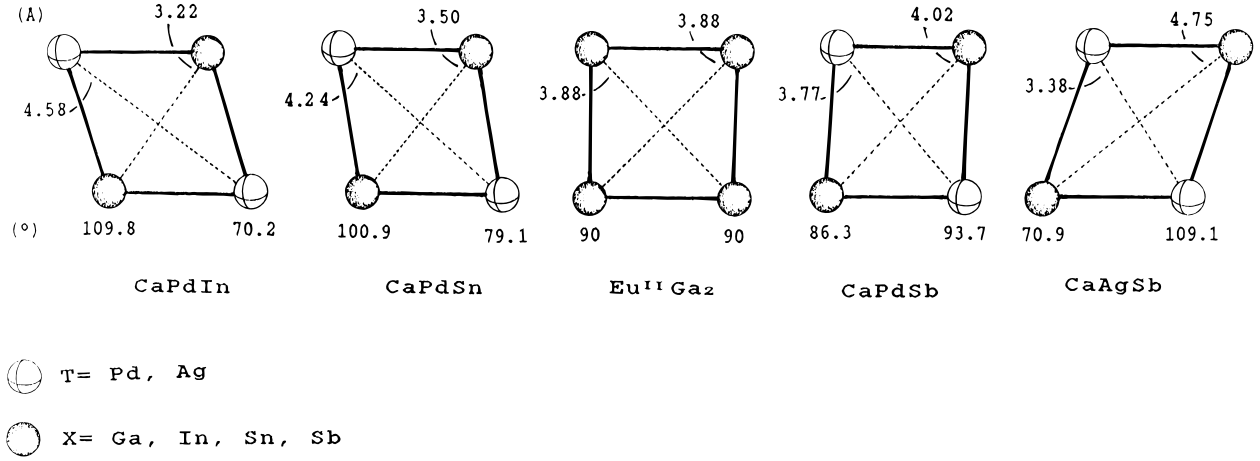

Figure 8. Comparison of some bond angles and distances for four MTX compounds and one MX_2 compound.

−0.08 Å,[50] giving an increase in the average bond length from 2.73 Å in CaPdSb to 2.80 Å (corrected) in CaAgSb. Using the Pauling equation[51]

$$d_{n'}(\text{Å}) = d_1(\text{Å}) - 0.60\ (\text{Å}) \log n'$$

gives a 20% decrease in the Pauling bond order (PBO) if the bond distance is increased from 2.73 Å (PBO = 1) to 2.80 Å (PBO = 0.8).

5. Bond Angles in MTX and MX_2 Phases

Nice trends are obvious in the bond angles for the distorted TX_4 and XT_4 tetrahedra presented in Table 3. Bond angles 213 and 214 (equal) always decrease in TX_4, but in general increase for XT_4. The same trend is found for the 215 bond angle.

The bond angles 315 and 415 (equal) for TX_4 and XT_4 are the angles that were originally fixed by symmetry at 90° in the $CeCu_2$ structure. In the TiNiSi structure the 315 and 415 (equal) angles in TX_4 sum up to 180° with the corresponding angles in XT_4 (e.g. for CaPdIn: 70.2° + 109.8° = 180°). In Figure 8, these bond angles are shown for a cluster of two T and two X atoms isolated from the MTX compounds CaPdIn, CaPdSn, CaPdSb, and CaAgSb (TiNiSi structure). They are compared with the analogous arrangement of four Ga atoms in $Eu^{II}Ga_2$ ($CeCu_2$ structure). $BaIn_2$ is too "large" to compare it with CaTX compounds, so the comparison is done using the "smaller" $Eu^{II}Ga_2$. Distances are also shown.

Figure 8 shows that the bond angles 315 and 415 (equal) in the XTX arrangement increase in the series CaPdIn, CaPdSn, $Eu^{II}Ga_2$, CaPdSb, and CaAgSb. The reverse is true for the bond angles 315 and 415 (equal) in the TXT arrangement, as it must be. This changes the parallelograms in Figure 8 from "left-tilted" for CaPdIn to "right-tilted" in CaAgSb.

The tilt observed is a consequence of increasing electronegativity (EN) in the 5sp main group series In, Sn, and Sb. The parallelograms tilt in order to maximize the distance (minimize the repulsion) between the more electronegative atoms.[34,52] For CaPdIn, where $EN_{Pd} > EN_{In}$, a left-tilted arrangement is built up (Figure 8), giving a Pd−Pd distance of 4.58 Å which is greater than the In−In distance of 3.22 Å. In CaPdSn this effect is lessened, since the electronegativity of Sn is greater than that of In and therefore closer to the electronegativity of Pd. In $Eu^{II}Ga_2$ (also $BaIn_2$), there is no reason for dispersion and the observed bond angles are 90°. Now right-tilting starts. In the compound CaPdSb, where $EN_{Sb} > EN_{Pd}$, the separation of the Sb atoms is 4.02 Å, in contrast to the Pd atoms, which are 3.77 Å apart. In CaAgSb the difference $EN_{Sb} - EN_{Ag}$ is greater than $EN_{Sb} - EN_{Ag}$; therefore the right-tilting increases, giving an Sb−Sb distance of of 4.75 Å.

Although the interpretation of the separation of atoms in the parallelograms is nicely consistent with an electronegativity argument, one must bear in mind that the distances (and therefore also the bond angles) are strongly dependent on the number of valence electrons, as was shown by the extended Hückel calculations in Section 2. Nevertheless, there is clearly a strong relationship between CaPdIn and CaAgSb on one side, and CaPdSn and CaPdSb on the other. Inspection of Figure 8 shows that the tilting of the parallelograms is nearly inverted: strong for CaPdIn and CaAgSb and weak for CaPdSn and CaPdSb.

Upon rotating the parallelograms of CaPdSb and CaAgSb by 180° around the Sb−Sb line (Figure 8), nearly the same parallelograms as in CaPdSn and in CaPdIn are obtained, but now with interchanged T and X positions! Inspection of Table 2 shows the structural reason for this phenomenon: the positional parameters of T and X atoms have been approximately interchanged in the two pairs CaPdIn/CaAgSb and CaPdSn / CaPdSb. Incredibly, the TiNiSi structure is able to vary the 315 and 415 (equal) XTX bond angle in the four-membered CaTX series from 70.2 to 79.1, 93.7, and 109.1°—a range of approximately 40°—by a single instruction: take the T and X positional parameters of the first two members and interchange them for the fourth and third member to X and T.

6. A Concluding Discussion of the TiNiSi Structural Type

The binary $CeCu_2$ and ternary TiNiSi structure are very versatile, accommodating a wide range of elements, electron counts, and geometrical features. Table 4 compares the number of known and structurally well characterized phases with those for the NaTl and the $CaIn_2$ structures.[2] The incidence of four-connected nets in binary and ternary compounds increases from the cubic (total: 37 phases) to the hexagonal (162) and then to the orthorhombic (408).

(49) The covalent radius of Pd (1.45 Å) has been calculated from that of Ag (1.528 Å) [47] and the relation of the fcc-metal−lattice parameters of Pd (3.8874 Å)[2] and of Ag (4.0853 Å).[2] 1.45 Å = 1.528 Å × 3.8874 /4.0853.

(50) Correction for bond distance Ag−Sb from CaAgSb to compare with bond distance Pd−Sb in CaPdSb is 1.45 − 1.528 Å = −0.08 Å (difference of the covalent radii of Pd and Ag).

(51) Pauling, L. *Die Natur der chemischen Bindung;* Verlag Chemie: Weinheim, Germany, 1964; p 240.

(52) Zheng, C.; Hoffmann, R.; Nesper, R.; von Schnering, H. G. *J. Am. Chem. Soc.* **1986**, *108*, 1876.

Table 4. Number of Binary and of Ternary Phases with 3D4C Nets[2]

	cubic	hexagonal	orthorhombic
structure	NaTl	$CaIn_2$	$CeCu_2$
binary phases	9	10	61
ternary phases	28	152	347[a]

[a] Counted: "all" 1:1:1 phases listed in ref 2.

In the cubic 3D4C net with the NaTl structure, there exist 9 binary compounds and 28 ternary compounds[2] with electron counts ranging from 6e (LiZn, LiCd; Li_2AgX with X = Al, Ga, In, Tl) to 9e (Li_2MgSb) (valence electron counts are for two tetrahedral atoms). To allow comparison with the $CeCu_2$ and the TiNiSi structure the valence electron count is converted to that for eight tetrahedral atoms; giving a range of electron counts from 24e to 36e for the binary and ternary NaTl phases. Since there are 18 compounds containing the small lithium atom (LiAl, LiGa, LiIn, LiZn, LiCd, and and 13 Li_2AX with A = Mg, Cu, Ag, Au), but only two containing the larger sodium atom (NaIn, NaTl), we conclude that the cubic 3D4C net is very sensitive to the size of the M^+ counterions. Due to the strong constraints of the cubic symmetry, it is not possible to increase the size of the cavities without increasing the bond lengths in the net.

The 3D4C hexagonal net with the $CaIn_2$ structure can do this better. Now both the c/a axial ratio of the lattice parameters and the positional parameter of the net ions can be varied. The net exists for Ga^-, In^-, and Tl^- ions (observed also for the NaTl structure) but with counterions M^{2+} increasing from the small Yb^{2+} and Ca^{2+}, to medium sized Sr^{2+}, and on to the large Ba^{2+}. Moreover 156 of 162 known binary and ternary phases adopting the $CaIn_2$ structure exist with 32 electrons. Thus, the $CaIn_2$ structure shows increased tolerance for geometrical distortions, but only allows a small degree of electronic variability.

The most versatile (most distortable) 3D4C net is the orthorhombic one. Up to 1991,[2] the binary $CeCu_2$ and the ternary TiNiSi structure were known for more than 400 phases. The structure has a great deal of flexibility, for consistent with its symmetry the following parameters may be changed: the three lattice parameters and their axial ratio; the positional parameters for the counterions; the positional parameters for the four-connected net ions; (for ternary phases the metal and main group elements may interchange); the number of valence electrons can range from 16 to 32e; (for MT_2 and MX_2 compounds with mono or divalent M, Table 1).

From our extended Hückel calculations it is concluded that the nature of the bonding in the binary Zintl-phases $SrAl_2$, $Eu^{II}Ga_2$, and $BaIn_2$ with the $CeCu_2$ structure is strongly related to that in the ternary phases CaTX (T = Pd, Pt; Ag; X = Al, Ga, In; Si, Ge, Sn; Sb) with the TiNiSi structure. The densities of states for $BaIn_2$ and CaPtSn show this clearly (Figures 2b and 7). For the CaTX phases with Pd(electron count: $d^{10} + 0$), Pt($d^{10} + 0$) and Ag($d^{10} + 1$) the filled d^{10} levels show up as large peaks with small dispersion well below the Fermi level. In addition, the calculations indicate that T−X bonding in the orthorhombic 3D4C net increases in strength up to a count of 30e per unit cell with four formula units and then weakens on going from 30 to 32e. Structural data, precisely derived on single crystals for the four-membered TiNiSi series of CaPdIn (20e), CaPdSn (24e), CaPdSb (28e), and CaAgSb (32e), confirm the results of the extended Hückel calculations. The general trends are observed for the compounds NaAuSn (24e), NaAuSb (28e), and NaCdSb (32e), too.

As shown above, the $CeCu_2$ and the TiNiSi structure can accommodate substantial geometrical and electronic stress. But the topological relation of these structures to the layers in black phosphorus indicates that they are sensitive to an increase in space filling. At 8 GPa black phosphorus is transformed into the more densely packed α-arsenic structure.[53] Therefore, 32-electron-phases with the $CeCu_2$ and TiNiSi structures at ambient pressure are probably good candidates for high pressure transformation into 3D4C nets with a topological relation to the α-arsenic structure!

Appendix

The program YAeHMOP ("Yet Another extended Hückel Molcular Orbital Package"), an extended Hückel implementation of the tight binding method written by G.L.,[19] was used in all calculations. Table 5 lists the parameters used for the various elements.

Table 5. Extended Hückel Parameters

	orbitals	H_{ii} (eV)	ζ_1	ζ_2	C_1	C_2
Ca	4s	−7.0	1.2			
	4p	−4.0	1.2			
Ba	6s	−4.76	1.263			
	6p	−2.64	1.263			
Na	3s	−5.1	0.733			
	3p	−3.0	0.733			
In	5s	−12.6	1.903			
	5p	−6.19	1.677			
Sn	5s	−16.16	2.12			
	5p	−8.32	1.82			
Pt	6s	−9.077	2.554			
	6p	−5.475	2.554			
	5d	−12.59	6.013	2.696	0.6334	0.5513

A 64 *k*-point set was used for the ideal indium-net of $BaIn_2$, 36 *k*-points for $CaIn_2$, 49 *k*-points for $BaIn_2$, 60 *k*-points for NaIn, and 27 *k*-points for CaPtSn. These mesh points in the irreducible wedge of the Brillouin zone were generated using the geometrical method of Ramirez and Böhm.[54]

IC9602557

(53) Jamieson, J. C. *Science* **1963**, *139*, 1291.
(54) Ramirez, R.; Böhm, M. C. *Int. J. Quantum Chem.* **1988**, *34*, 571.